

Metal–Metal Bonding in Tetracyanometalates (M = Pt^{II}, Pd^{II}, Ni^{II}) of Monovalent Thallium. Crystallographic and Spectroscopic Characterization of the New Compounds Tl₂Ni(CN)₄ and Tl₂Pd(CN)₄

Mikhail Maliarik,^{*,†} Jeffrey K. Nagle,[‡] Andrey Ilyukhin,[§] Elena Murashova,^{||} János Mink,^{⊥,#} Mikhail Skripkin,[○] Julius Glaser,[◆] Margit Kovacs,[▽] and Attila Horváth[▽]

IFM-Department of Chemistry, Linköping University, SE-581 83 Linköping, Sweden, Department of Chemistry, Bowdoin College, Brunswick, Maine 04011-8466, Kurnakov Institute of General and Inorganic Chemistry, Russian Academy of Science, Leninsky Prospect 31, 119991 Moscow, Russia, Chemistry Department of M. V. Lomonosov, Moscow State University, Leninskie Gori 1, 119992 Moscow, Russia, Department of Molecular Spectroscopy, Chemical Research Center of the Hungarian Academy of Sciences, P.O. Box 77, H-1525 Budapest, Hungary, Faculty of Information Technology, Research Institute of Chemical and Process Engineering and Analytical Chemistry Research Group of the Hungarian Academy of Sciences, University of Pannonia, P.O. Box 158, Veszprém, Hungary, Department of Chemistry, St. Petersburg State University, Universitetskii pr. 26, 198504 St. Petersburg, Russia, Department of Chemistry, The Royal Institute of Technology (KTH), S-100 44 Stockholm, Sweden, and Department of General and Inorganic Chemistry, University of Pannonia, Pf. 158, H-8201, Veszprém, Hungary

Received November 2, 2006

The new crystalline compounds Tl₂Ni(CN)₄ and Tl₂Pd(CN)₄ were synthesized by several procedures. The structures of the compounds were determined by single-crystal X-ray diffraction. The compounds are isostructural with the previously reported platinum analogue, Tl₂Pt(CN)₄. A new synthetic route to the latter compound is also suggested. In contrast to the usual infinite columnar stacking of [M(CN)₄]²⁻ ions with short intrachain M–M separations, characteristic of salts of tetracyanometalates of Ni^{II}, Pd^{II}, and Pt^{II}, the structure of the thallium compounds is noncolumnar with the two Tl^I ions occupying axial vertices of a distorted pseudo-octahedron of the transition metal, [MTl₂C₄]. The Tl–M distances in the compounds are 3.0560(6), 3.1733(7), and 3.140(1) Å for Ni^{II}, Pd^{II}, and Pt^{II}, respectively. The short Tl–Ni distance in Tl₂Ni(CN)₄ is the first example of metal–metal bonding between these two metals. The strength of the metal–metal bonds in this series of compounds was assessed by means of vibrational spectroscopy. Rigorous calculations, performed on the molecules in *D*_{4h} point group symmetry, provide force constants for the Tl–M stretching vibration constants of 146.2, 139.6, and 156.2 N/m for the Ni^{II}, Pd^{II}, and Pt^{II} compounds, respectively, showing the strongest metal–metal bonding in the case of the Tl–Pt compound. Amsterdam density-functional calculations for isolated Tl₂M(CN)₄ molecules give Tl–M geometry-optimized distances of 2.67, 2.80, and 2.84 Å for M = Ni^{II}, Pd^{II}, and Pt^{II}, respectively. These distances are all substantially shorter than the experimental values, most likely because of intermolecular Tl–N interactions in the solid compounds. Time-dependent density-functional theory calculations reveal a low-energy, allowed transition in all three compounds that involves excitation from an a_{1g} orbital of mixed Tl 6p_z–M nd_{z²} character to an a_{2u} orbital of dominant Tl 6p_z character.

Introduction

The crystal structure of Tl₂Pt(CN)₄¹ was among the first reported examples of metal–metal-bonded compounds involving a thallium atom. The compound has attracted significant interest because its crystal structure does not

possess the usual infinite columnar stacking of [Pt(CN)₄]²⁻ ions with short intrachain Pt–Pt distances (3.09–3.75 Å)

* To whom correspondence should be addressed. E-mail: misha@ifm.liu.se.

[†] Linköping University.

[‡] Bowdoin College.

[§] Kurnakov Institute of General and Inorganic Chemistry, Russian Academy of Science.

^{||} Moscow State University.

[⊥] Chemical Research Center of the Hungarian Academy of Sciences.

[#] Hungarian Academy of Sciences, University of Pannonia.

[○] St. Petersburg State University.

[◆] The Royal Institute of Technology.

[▽] Department of General and Inorganic Chemistry, University of Pannonia.

found in the alkali, alkaline-earth, and rare-earth salts of tetracyanoplatinate(II).² In the case of the thallos compound, the two Tl^I ions occupy trans positions of a platinum pseudo-octahedron ($[PtTl_2C_4]$) instead, with $Pt-Tl$ separations of 3.14 Å.¹ Density-functional calculations of the compound show that interaction between Tl^I and $[Pt(CN)_4]^{2-}$ moieties is primarily ionic in nature but with a sizable covalent character.³ More recent second-order Møller–Plesset-level calculations of the same compound have also revealed a pronounced heterometallic interaction.⁴ This is, however, overcompensated by a sizable electrostatic lengthening of the $Pt-Tl$ bond in the solid due to crystal-field effects. An intermetallic $Pt-Tl$ distance of 2.877 Å was calculated for the free $Tl_2Pt(CN)_4$ molecule.

The crystal structures of tetracyanometalates of nickel(II) and palladium(II) are similar to that of $[Pt(CN)_4]^{2-}$. Usually, square-planar ions $[M(CN)_4]^{2-}$ ($M = Ni, Pd$) form a polymeric structure with infinite $-M-M-M-$ chains.⁵ The separations between the metal atoms are in the ranges of 3.31–3.39 and 3.34–3.80 Å for nickel and palladium salts, respectively. Water molecules of crystallization play an important role in stabilizing the columnar structure by means of hydrogen bonding. When no water molecules are present in the crystal lattice, as in the anhydrous structures of $K_2[Ni(CN)_4]$ ^{6a} and $CsK[Ni(CN)_4]$,^{6b} the intermetallic distances in the chains increase up to 4.29–4.55 Å. However, in the structure of $[Et_2NH_2]_2[Pd(CN)_4]$, with extensive hydrogen bonding between cations and anions, the distance between the palladium ions is substantially longer, 6.35 Å, compared with the $Pd \cdots Pd$ separations in the inorganic salts of the $[Pd(CN)_4]^{2-}$ anion, and the columnar structure is lost.⁷ This is attributed to the size of the cation.

The crystallization of tetracyanometalates with “bulky” counterions, such as $[Cd(NH_3)_2]^{2+}$,^{8a} $[Cd(H_2O)_2]^{2+}$,^{8b} $[Co(H_2O)_2]^{2+}$,⁹ $[Fe(H_2O)_2]^{2+}$,¹⁰ and $[Ni(en)_2]^{2+}$,¹¹ prevents the formation of linear $-M-M-M-$ chains as well. In this case, the cyano groups of the $[M(CN)_4]^{2-}$ ions bridge the two heterometals and a layered structure is formed. A large class of Hofmann-type clathrate structures, $M(NH_3)_2M'(CN)_4 \cdot 2G$ ($M = Ni^{2+}, Pd^{2+}, Pt^{2+}$; $G =$ various organic guest mol-

ecules), are also known.¹² In these inclusion compounds, the multidimensional framework of the hosts is comprised of the linear $M'-CN-M$ linkages, whereas no direct contacts between the M' atoms occur (see ref 13 and references cited therein).

No crystal structures of the Tl^+ salts of either $[Ni(CN)_4]^{2-}$ or $[Pd(CN)_4]^{2-}$ have been reported so far. Bok and Leipoldt reported the synthesis of $Tl_2Pd(CN)_4$, but the information obtained was restricted to results from elemental analysis and X-ray powder diffraction studies.¹⁴ In this paper, we present the synthesis and X-ray crystal structure determination of tetracyanometalate compounds of nickel(II) and palladium(II) with monovalent thallium. Both salts belong to the family of isostructural compounds $Tl_2M(CN)_4$ ($M = Ni, Pd, Pt$) and have noncolumnar structures with linear $Tl-M-Tl$ entities. In addition, a comparative study of the vibrational spectra of the family of compounds is reported. The force constants in the molecules are calculated and discussed with the primary focus on the strength of the metal–metal bond. Amsterdam density-functional (ADF)¹⁵ and density-functional theory (DFT) calculations of optimized geometries and vibrational frequencies, together with time-dependent DFT (TDDFT) calculations of excitation energies, are reported for comparison with experimental results.

Experimental Section

Materials and Solutions. Potassium tetracyanonickelate(II) hydrate was prepared according to a general procedure that includes precipitation of the sparingly soluble nickel(II) cyanide¹⁶ followed by its dissolution in a 2-fold molar excess of an aqueous solution of potassium cyanide. A crystalline compound of composition $K_2Ni(CN)_4 \cdot H_2O$ was obtained after slow evaporation of the solvent. The salt was recrystallized from water. Palladium(II) cyanide ($Pd(CN)_2$, Chempur, reagent grade) and platinum(II) cyanide ($Pt(CN)_2$, Alfa, reagent grade) were used without further purification. An aqueous solution of thallium(I) hydroxide was prepared by the reaction between aqueous solutions of Tl_2SO_4 and BaO followed by the filtration of precipitated $BaSO_4$. An aqueous solution of thallium(I) cyanide was prepared via cation exchange with potassium in an aqueous solution of KCN .¹⁷ The solutions were analyzed for Tl^+ as described previously.¹⁸

$Tl_2Ni(CN)_4$, Method 1. An aqueous solution of $Tl_2Ni(CN)_4$ was prepared by passing 4 mL of an aqueous solution of potassium

- (1) Nagle, J. K.; Balch, A. L.; Olmstead, M. M. *J. Am. Chem. Soc.* **1988**, *110*, 319–321.
- (2) Gielmann, G.; Yershin, H. *Struct. Bonding (Berlin)* **1985**, *62*, 87–153.
- (3) Ziegler, T.; Nagle, J. K.; Snijders, J. G.; Baerends, E. J. *J. Am. Chem. Soc.* **1989**, *111*, 5631–5635.
- (4) Dolg, M.; Pyykkö, P.; Runeberg, N. *Inorg. Chem.* **1996**, *35*, 7450–7451.
- (5) Sharpe, A. G. *The Chemistry of Cyano Complexes of the Transition Metals*; Academic Press: London, 1976.
- (6) (a) Vannenberg, R. G. *Acta Chem. Scand.* **1964**, *18*, 2385. (b) Musselman, R. G.; Stecher, L. C.; Watkins, S. *Inorg. Chem.* **1980**, *19*, 3400.
- (7) Jerome-Lerutte, S. *Acta Crystallogr.* **1971**, *B 27*, 1624–1630.
- (8) (a) Cernak, J.; Kappenstein, C. *Collect. Czech. Chem. Commun.* **1987**, *52*, 1915. (b) Ham, W. K.; Weakly, T. C. R.; Page, C. J. *J. Solid State Chem.* **1993**, *107*, 101.
- (9) Niu, T.; Crisci, G.; Lu, J.; Jacobson, A. J. *Acta Crystallogr., Sect. C* **1998**, *54*, 565–567.
- (10) (a) Kitazawa, T.; Fukunaga, M.; Takahashi, M.; Takeda, M. *Mol. Cryst. Liq. Cryst.* **1994**, *244*, 331–336. (b) Yuge, H.; Kim, C.-H.; Iwamoto, T.; Kitazawa, T. *Inorg. Chim. Acta* **1997**, *257*, 217–224.
- (11) Ruegg, M.; Ludi, A. *Theor. Chim. Acta* **1971**, *20*, 193.

- (12) (a) Iwamoto, T. In *Inclusion Compounds*; Atwood, J. L., Davies, J. E. D., MacNicol, D. D., Eds.; Oxford University Press: Oxford, 1991; Vol. 5, pp 177–212. (b) Most of the crystal structures were reported for the case of $M' = Ni$, but Pd and Pt compounds were shown to be isostructural.
- (13) Iwamoto, T. In *Comprehensive Supramolecular Chemistry*; MacNicol, D. D., Toda, F., Bishop, R., Eds.; Pergamon Press: Oxford, 1996; Vol. 6, pp 643–690.
- (14) Bok, V. L. D. C.; Leipoldt, J. G. *Z. Anorg. Allg. Chem.* **1966**, *344*, 86–91.
- (15) (a) *ADF: Density Functional Theory (DFT) Software for Chemists*; Scientific Computing & Modeling: Amsterdam. (b) te Velde, G.; Bickelhaupt, F. M.; van Gisbergen, S. J. A.; Fonseca Guerra, C.; Baerends, E. J.; Snijders, J. G.; Ziegler, T. *J. Comput. Chem* **2001**, *22*, 931.
- (16) Elemental analysis of the precipitate corresponds to a dihydrate compound, $Ni(CN)_2 \cdot 2H_2O$.
- (17) Penneman, R. A.; Staritzky, E. *J. Inorg. Nucl. Chem.* **1958**, *6*, 112–118.
- (18) Blixt, J.; Györi, B.; Glaser, J. *J. Am. Chem. Soc.* **1989**, *111*, 7784.

tetracyanonickelate(II) monohydrate (0.155 M) through a large (10-fold) excess of cation exchanger (Dowex-50) in the thallium(I) form (the Tl^+ -form resin was prepared by titrating a slurry of a H^+ -form resin with a TIOH solution until a slight permanent alkalinity was observed¹⁷). Bright yellow-orange crystals of $\text{Tl}_2\text{Ni}(\text{CN})_4$ were obtained by slow evaporation of water. The solid was recrystallized. Anal. Calcd for $\text{Tl}_2\text{NiC}_4\text{N}_4$ (517.6): C, 8.4; N, 9.8. Found: C, 8.4; N, 9.7.

Method 2. A solution of $\text{Tl}_2\text{Ni}(\text{CN})_4$ was prepared by the reaction between an aqueous solution of TICN (0.047 M) and solid $\text{Ni}(\text{CN})_2 \cdot 2\text{H}_2\text{O}$. A thallos cyanide solution (0.047 M, 102 mL) was added to the excess of the sparingly soluble powder of $\text{Ni}(\text{CN})_2 \cdot 2\text{H}_2\text{O}$ (3.9 mmol) under intensive stirring at room temperature.¹⁹ The nonreacted $\text{Ni}(\text{CN})_2 \cdot 2\text{H}_2\text{O}$ was separated from the solution by suction filtration. Bright yellow-orange crystals of $\text{Tl}_2\text{Ni}(\text{CN})_4$ were obtained by slow evaporation of the solvent. The solid was recrystallized. Powder X-ray analysis of the polycrystalline samples of the compound obtained from two syntheses was carried out. The analyses showed their structure to be identical with that of single crystals of $\text{Tl}_2\text{Ni}(\text{CN})_4$ (see the Supporting Information).

$\text{Tl}_2\text{Pd}(\text{CN})_4$. An aqueous solution of $\text{Tl}_2\text{Pd}(\text{CN})_4$ was prepared by a reaction between aqueous TICN (0.125 M) and solid $\text{Pd}(\text{CN})_2$. The sparingly soluble powder of $\text{Pd}(\text{CN})_2$ (0.5 mmol) was completely dissolved by the addition of 8 mL of TICN solution (1.0 mmol) under intensive stirring at room temperature. Colorless crystals of $\text{Tl}_2\text{Pd}(\text{CN})_4$ were obtained by slow evaporation of the solvent. Anal. Calcd for $\text{Tl}_2\text{PdC}_4\text{N}_4$ (619.3): C, 7.8; N, 9.0. Found: C, 7.8; N, 8.7.

$\text{Tl}_2\text{Pt}(\text{CN})_4$. Two preparative routes for synthesis of the compound were described previously. Slow diffusion of aqueous TlNO_3 into aqueous $\text{K}_2\text{Pt}(\text{CN})_4 \cdot 3\text{H}_2\text{O}$ was used to yield sparingly soluble colorless crystals of $\text{Tl}_2\text{Pt}(\text{CN})_4$.¹ The compound, with the same lattice parameters but a pale-yellow color, was obtained by mixing aqueous solutions of $\text{BaPt}(\text{CN})_4$ and Tl_2SO_4 followed by removal of the BaSO_4 precipitate and crystallization of $\text{Tl}_2\text{Pt}(\text{CN})_4$.²⁰ It was suggested that the yellow color of the latter form arose from impurities that did not affect the crystallographic or main optical characteristics of the compound but resulted in the appearance of additional emission bands. In this work, $\text{Tl}_2\text{Pt}(\text{CN})_4$ was prepared by a different procedure, namely, by reaction between aqueous TICN (0.170 M) and solid $\text{Pt}(\text{CN})_2$. The sparingly soluble $\text{Pt}(\text{CN})_2$ powder (0.7 mmol) was completely dissolved upon the addition of 8.2 mL of TICN (1.4 mmol) under intensive stirring at room temperature. Pale-yellow needle-shaped crystals were obtained by slow evaporation of the solvent. Powder X-ray analyses of the compound revealed it to be identical with $\text{Tl}_2\text{Pt}(\text{CN})_4$ (see the Supporting Information). Anal. Calcd for $\text{Tl}_2\text{PtC}_4\text{N}_4$ (708): C, 6.8; N, 7.9. Found: C, 6.8; N, 7.8.

Single-Crystal and Powder X-ray Analyses. The data collection for the crystals $\text{Tl}_2\text{Ni}(\text{CN})_4$ (**1**) and $\text{Tl}_2\text{Pd}(\text{CN})_4$ (**2**) was performed on Syntex P2₁ and STOE IPDS diffractometers, respectively. The *SHELXS97* program^{21a} was used to solve the structures, and the *SHELXL97* program^{21b} was used to refine the structures of **1** and **2**. Selected crystallographic and experimental data together with

Table 1. Crystallographic Parameters for the Isostructural Compounds $\text{Tl}_2\text{M}(\text{CN})_4$ (M = Ni, Pd, Pt) and Data Collection Details for $\text{Tl}_2\text{Ni}(\text{CN})_4$ and $\text{Tl}_2\text{Pd}(\text{CN})_4$

	chemical formula		
	$\text{Tl}_2\text{Ni}(\text{CN})_4$	$\text{Tl}_2\text{Pd}(\text{CN})_4$	$\text{Tl}_2\text{Pt}(\text{CN})_4^a$
<i>a</i> , Å	6.154(2)	6.277(2)	6.325(2)
<i>b</i> , Å	7.282(1)	7.437(2)	7.386(2)
<i>c</i> , Å	9.396(3)	9.591(3)	9.581(3)
β , deg	104.29(1)	104.67(1)	104.92
<i>V</i> , Å ³	408.0(2)	433.1(2)	432.5(2)
<i>Z</i>	2	2	2
cryst syst	monoclinic	monoclinic	monoclinic
space group	$P2_1/n$ (No. 14)	$P2_1/n$ (No. 14)	$P2_1/n$ (No. 14)
diffractometer	Syntex P2 ₁ ^b	STOE IPDS ^c	
λ (Mo K α), Å	0.71073	0.71073	
<i>T</i> , K	295	293(2)	
<i>fw</i>	571.53	619.22	
<i>D_c</i> (g/cm ³)	4.652	4.748	
μ (mm ⁻¹)	41.611	39.103	
R1 ($F_o > 4\sigma(F_o)$)	0.0374	0.0285	
R1 (all data)	0.0376	0.0440	
wR2 ($F_o > 4\sigma(F_o)$)	0.0982	0.0428	
wR2 (all data)	0.0983	0.0446	
GOFF	1.074	1.266	

^a Reported in ref 1. ^b Utilizing a $\omega/2\theta$ scan. ^c A total of 100 area detector images from $\varphi = 0^\circ$ to 200° in steps of 2.0° and with a measuring time of 6 min were collected.

Table 2. Selected Bond Lengths (Å) in the Structures of $\text{Tl}_2\text{Ni}(\text{CN})_4$ and $\text{Tl}_2\text{Pd}(\text{CN})_4^a$

$\text{Tl}_2\text{Ni}(\text{CN})_4$		$\text{Tl}_2\text{Pd}(\text{CN})_4$	
Tl(1)–N(2)#1	2.838(10)	Tl(1)–N(2)#1	2.847(10)
Tl(1)–N(2)#2	2.856(10)	Tl(1)–N(2)#2	2.853(11)
Tl(1)–N(1)#3	2.938(12)	Tl(1)–N(1)#3	2.963(9)
Tl(1)–N(1)#4	2.978(11)	Tl(1)–N(1)#4	2.975(11)
Tl(1)–N(1)#5	3.019(11)	Tl(1)–N(1)#5	3.057(11)
Tl(1)–Ni(1)#6	3.0560(6)	Tl(1)–Pd(1)#6	3.1733(7)
Ni(1)–C(1)	1.885(10)	Pd(1)–C(1)	1.985(11)
Ni(1)–C(2)	1.843(10)	Pd(1)–C(2)	2.009(11)
C(1)–N(1)	1.150(15)	C(1)–N(1)	1.180(14)
C(2)–N(2)	1.173(13)	C(2)–N(2)	1.126(13)

^a Symmetry transformations used to generate equivalent atoms follow: #1, $x - 1/2, -y + 1/2, z + 1/2$. #2, $-x + 1/2, y - 1/2, -z + 3/2$. #3, $x, y - 1, z + 1$. #4, $-x + 1, -y + 1, -z + 1$. #5, $-x + 1/2, y - 1/2, -z + 1/2$. #6, $x, y, z + 1$.

the refinement details are given in Table 1. Selected bond lengths and angles in the structures of compounds **1** and **2** are given in Table 2 and Table 3, respectively. X-ray powder diffraction data on compounds **1** and **2** as well as $\text{Tl}_2\text{Pt}(\text{CN})_4$ (**3**) were obtained from a Philips PW 1710 diffractometer, $\lambda = 1.54060$ Å (Cu K α_1 , germanium monochromator); cf. Figure S1 in the Supporting Information.

Vibrational Spectroscopy. Raman spectra were measured by means of the FT-Raman accessory of a Bio-RAD FTS 6000 FT-IR spectrometer. The 1064 nm line from a Spectra-Physics Nd:YAG laser was used to irradiate the sample with about 150 mW of power. The mid-infrared absorption spectra were obtained by means of a Perkin-Elmer 1725 FT-IR spectrometer. Mulls in Nujol enclosed in BaF₂ windows were used for the measurements. The far-infrared spectra were recorded by means of a Bio-Rad FTS 6000 FT-IR spectrometer; the samples were pressed into polyethylene disks. The observed wavenumbers for the compounds $\text{Tl}_2\text{M}(\text{CN})_4$ (M = Ni, Pd, Pt) are presented in Table 4.

Both $\text{Tl}_2\text{M}(\text{CN})_4$ molecules and $[\text{M}(\text{CN})_4]^{2-}$ ions in $\text{K}_2[\text{M}(\text{CN})_4]$ possess D_{4h} symmetry. Wilson's GF matrix method was used for the calculation of vibrational frequencies using a symmetrized

(19) To ensure formation of the tetra cyano species and avoid formation of the penta cyano complex (see, e.g., ref 5), cyanide ions were taken in deficit compared with the metal salt.

(20) Weissbart, B.; Balch, A. L.; Tinti, D. S. *Inorg. Chem.* **1993**, *32*, 2096–2103.

(21) (a) Sheldrick, G. M. *SHELXS97, Computer Program for the Solution of Crystal Structures*, release 97-2; University of Göttingen: Göttingen, Germany, 1997. (b) Sheldrick, G. M. *SHELXL97, Computer Program for the Refinement of Crystal Structures*, release 97-2; University of Göttingen: Göttingen, Germany, 1997.

Table 3. Bond Angles (deg) in the Structures of $Tl_2Ni(CN)_4$ and $Tl_2Pd(CN)_4$ ^a

$Tl_2Ni(CN)_4$		$Tl_2Pd(CN)_4$	
C(1)#7–Ni(1)–C(1)	180	C(2)#7–Pd(1)–C(2)	180
C(2)–Ni(1)–C(2)#7	180	C(2)#7–Pd(1)–C(1)	89.7(4)
C(2)–Ni(1)–C(1)#7	89.5(5)	C(2)–Pd(1)–C(1)	90.3(4)
C(2)#7–Ni(1)–C(1)#7	90.5(5)	C(2)#7–Pd(1)–C(1)#7	90.3(4)
C(2)–Ni(1)–C(1)	90.5(5)	C(2)–Pd(1)–C(1)#7	89.7(4)
C(2)#7–Ni(1)–C(1)	89.5(5)	C(1)–Pd(1)–C(1)#7	180
C(2)–Ni(1)–Tl(1)#8	92.0(3)	C(2)#7–Pd(1)–Tl(1)#8	87.0(3)
C(2)#7–Ni(1)–Tl(1)#8	88.0(3)	C(2)–Pd(1)–Tl(1)#8	93.0(3)
C(1)#7–Ni(1)–Tl(1)#8	87.6(3)	C(1)–Pd(1)–Tl(1)#8	93.2(3)
C(1)–Ni(1)–Tl(1)#8	92.4(3)	C(1)#7–Pd(1)–Tl(1)#8	86.8(3)
C(2)–Ni(1)–Tl(1)#9	88.0(3)	C(2)#7–Pd(1)–Tl(1)#9	93.0(3)
C(2)#7–Ni(1)–Tl(1)#9	92.0(3)	C(2)–Pd(1)–Tl(1)#9	87.0(3)
C(1)#7–Ni(1)–Tl(1)#9	92.4(3)	C(1)–Pd(1)–Tl(1)#9	86.8(3)
C(1)–Ni(1)–Tl(1)#9	87.6(3)	C(1)#7–Pd(1)–Tl(1)#9	93.2(3)
Tl(1)#8–Ni(1)–Tl(1)#9	180	Tl(1)#8–Pd(1)–Tl(1)#9	180
N(1)–C(1)–Ni(1)	175.6(11)	N(1)–C(1)–Pd(1)	178.6(10)
N(2)–C(2)–Ni(1)	178.1(10)	N(2)–C(2)–Pd(1)	179.7(11)

^a Symmetry transformations used to generate equivalent atoms follow: #7, $-x, -y + 1, -z$. #8, $x, y, z - 1$. #9, $-x, -y + 1, -z + 1$.

valence force field. The initial force constants were adopted from Kubas and Jones²² and refined to give a satisfactory fit of calculated and observed frequencies (see Table 5). The PC-based program package developed by Mink and Mink²³ was used for the calculations. Calculated force constants for the series of compounds $Tl_2M(CN)_4$ are presented in Table 6. The calculations were also carried out on the parent compounds $K_2M(CN)_4$ ($M = Ni, Pd, Pt$) using the frequency values obtained in the current work. The results are shown in Table 7 and are in good agreement with the data calculated in ref 22.

Computations. DFT and TDDFT calculations were performed with a 2000 development version of ADF at the Free University of Amsterdam and a Mac OS-X 2006.01 commercial version of ADF¹⁵ at Bowdoin College. All ADF geometry optimization and vibrational frequency calculations included scalar relativistic effects through the ZORA method,²⁴ Becke–Perdew exchange–correlation potentials,²⁵ and all-electron QZ4P basis sets from the ADF basis sets library for all atoms. The SAOP XC functional²⁶ was used for the TDDFT calculation of the excitation energies. All calculations were done with geometries constrained to D_{4h} symmetry. Spin–orbit coupling and aqueous solvation effects were included in some ADF 2006.01 calculations (solvation effects incorporated through the COSMO feature of ADF provide a simple way of mimicking Tl–N interactions in these compounds without lowering the molecular symmetry from D_{4h}).

Luminescence Spectroscopy. Luminescence excitation and emission (steady-state and time-resolved) spectra of the polycrystalline samples of the compounds $Tl_2M(CN)_4$ ($M = Ni, Pd$) were obtained with a Perkin-Elmer LS50B spectrometer using a sample holder developed for powders. The excitation of the samples in the time-resolved study was performed with the third harmonic of

the Nd:YAG laser (355 nm) with a pulse width of 5 ns. Excitation and emission spectra of the polycrystalline samples of the compounds suspended in glycerol at 298 K were obtained with a Hitachi F-4500 fluorescence spectrometer.

UV–Vis Measurements. Absorption spectra of the compounds $Tl_2M(CN)_4$ ($M = Ni, Pd$) as crystalline suspensions in glycerol were obtained using a Hitachi 2001 UV–vis spectrophotometer. Quartz cuvettes with a 1.0 cm path length were used.

Results and Discussion

Crystal Structures of the $Tl_2M(CN)_4$ ($M = Ni, Pd, Pt$) Salts. The thallium(I) salts of tetracyanometalates(II) of nickel and palladium are isostructural with $Tl_2Pt(CN)_4$ ¹ (Table 1). This implies that bonding interactions between thallos ion and $[M(CN)_4]^{2-}$ entities in the compounds exclude any short $M\cdots M$ contacts between the transition-metal atoms. The coordination environment of the transition-metal atom in the compounds can be described as a pseudo-octahedron: four carbon atoms of the cyanide groups form a slightly distorted equatorial plane, while two thallium atoms occupy axial vertices of the polyhedron (the M atom lies at the inversion center and the Tl–M–Tl angle is 180°) (see Figure 1 and Table 3). Both the M–C bond lengths (1.843–1.885, 1.985–2.009, and 2.000–2.010 Å for Ni, Pd, and Pt, respectively) and C–N separations in the C–N groups (1.150–1.173, 1.126–1.180, and 1.155–1.162 Å for Ni, Pd, and Pt, respectively) fall within the range of distances known for M^{II} –cyano ($M = Ni, Pd, Pt$) compounds (Table 2).^{5,27} The thallium atoms in all three structures have strongly distorted pseudo-octahedral coordination formed by the five nitrogen atoms of the cyano groups and a transition-metal atom (Figure 2). The Tl–N bond lengths in the polyhedron (2.84–3.02, 2.85–3.06, and 2.80–3.04 Å for Ni, Pd, and Pt, respectively) are characteristic of compounds of monovalent thallium (Table 2) (see, e.g., ref 28).

It is natural to suppose that the noncolumnar structures of the $Tl_2M(CN)_4$ ($M = Ni, Pd, Pt$) compounds with short M–Tl separations are caused by metal–metal bonding. The stabilization of a linear, trinuclear Tl–M–Tl entity can be attributed to σ bonding involving primarily the empty $6p_z$ and filled $6s$ orbitals on the two thallium ions and the empty $(n + 1)p_z$ and filled nd_z^2 orbitals of the transition-metal ions (see refs 1 and 3 and vide infra).

Tl–M Distances. An important feature of the family of the $Tl_2M(CN)_4$ compounds is a thallium–transition-metal bond distance. The Tl–M separations are 3.0560, 3.1733, and 3.140 Å for Ni, Pd, and Pt, respectively (Table 2). The longest Tl–M bond is found for the palladium compound. The lack of monotonic increase of the Tl–M distance along the group 10 metals in the series of isostructural compounds

(22) Kubas, G. J.; Jones, L. H. *Inorg. Chem.* **1974**, *13*, 2816–2819.

(23) Mink, J.; Mink, L. M. *Computer Program System for Vibrational Analyses of Polyatomic Molecules*; available from J. Mink, Department of Analytical Chemistry, Veszprém University, P.O. Box 158, H-8201 Veszprém, Hungary.

(24) van Lenthe, E.; Ehlers, A. E.; Baerends, E. J. *J. Chem. Phys.* **1999**, *110*, 8943.

(25) (a) Becke, A. *Phys. Rev. B: Condens. Matter Mater. Phys.* **1986**, *38*, 3098. (b) Perdew, J. P. *Phys. Rev. B: Condens. Matter Mater. Phys.* **1986**, *33*, 8822 (Erratum *Phys. Rev. B: Condens. Matter Mater. Phys.* **1986**, *34*, 7406).

(26) Schipper, P. R. T.; Gritsenko, O. V.; van Gisbergen, S. J. A.; Baerends, E. J. *J. Chem. Phys.* **2000**, *112*, 1344.

(27) (a) Sharpe, A. G. In *Comprehensive Coordination Chemistry*; Wilkinson, G.; Gillard, R. D.; McCleverty, J. A., Eds.; Pergamon Press: Oxford, 1987; Vol. 2, pp 7–14. (b) Golub, A. M.; Köller, H.; Skopenko, V. V. *Chemistry of Pseudohalides*; Elsevier: Amsterdam, 1986.

(28) (a) Blom, N.; Ludi, A.; Burgi, H.-B.; Tichy, K. *Acta Crystallogr.* **1984**, *C40*, 1767–1769. (b) Omary, M. A.; Webb, T. R.; Assefa, Z.; Shankle, G. E.; Patterson, H. H. *Inorg. Chem.* **1998**, *37*, 1380–1386. (c) Johnson, M. T.; Campana, C. F.; Foxman, B. M.; Desmarais, W.; Vela, M. J.; Miller, J. S. *Chem.–Eur. J.* **2000**, *6*, 1805–1810.

Table 4. Experimental Vibrational Bands for $Tl_2M(CN)_4$ Species and Their Tentative Assignments^{a,b}

$Tl_2Ni(CN)_4$		$Tl_2Pd(CN)_4$		$Tl_2Pt(CN)_4$		assignment
IR	Raman	IR	Raman	IR	Raman	
	2532 vvw					3135 + 409
2160 vw	2135 vs 2119 vs		2151 vs 2133 vs		2157 vs 2136 vs	A_{1g} , ν_1 , CN sym str B_{1g} , ν_5 , CN str
2127 vs 2122 vs		2138 vs 2122 vs		2140 vs 2122 vs		E_u , ν_{16} , CN asym str ^c E_u , ν_{16} , CN asym str ν_{16} , $^{12}C^{15}N$ asym str ν_{16} , $^{13}C^{14}N$ asym str ν_{16} , $^{13}C^{14}N$ asym str
2081 vw 2066 vw 533 w	2081 vw 2066 vw	(2091 vw) (2078 vw)	2108 vvw 2094 vw 2081 vw		2110 vvw 2094 vw 2081 vw	370 + 173 413 + 116 413 + 83
510 vw		477 vw		512 vw 492 sh 486 m		E_u , ν_{17} , MCN out-of-plane lin bend
	482 vw			455 sh	457 w	370 + 114 303 + 160 310 + 142
448 sh			384 w	443 vw		303 + 146 B_{2g} , ν_7 , MCN out-of-plane lin bend
422 s, sh	431 sh	430 w		469 m	413 w	A_{2u} , ν_{11} , MCN in-plane lin bend
			427 m	455 sh		303 + 124 328 + 83 310 + 114
413 vs	417 sh 409 m	384 vs	430 m 413 sh,w	409 vs	479 m	E_u , ν_{18} , MC str A_{1g} , ν_2 , MC sym str 303 + 129 303 + 87
391 sh		392 sh 372 sh		~360 sh		
338 w, sh	370 vvw 329 w 313 sh 310 m		392 w		488 w 333 sh	B_{1g} , ν_6 , MC str 173 + 161 2×161
			303 m		328 m	E_g , ν_9 , MCN in-plane lin bend
204 sh 175 m, sh	211 vvw		299 sh	295 sh		160 + 138 120 + 96
	173 m 170 sh	171 sh	160 sh	180 m, sh	187 sh	
158 m 153 m, sh 145 m, sh		154 sh 146 m		152 sh 145 m		A_{2u} , ν_{12} , MTL asym str
135 w, sh	142 s	135 m, sh	138 s		142 s	A_{1g} , ν_3 , MTL sym str E_u , ν_{19} , CMC deform
120 m 117 m		119 m		124 sh 116 s 102 m	101 m	A_{2u} , ν_{13} , TIMC deform
82 m 70 m	96 s 86 sh		102 m 87 m		83 m	E_g , ν_{10} , TIMC deform
41 w	50 w 41 sh 36 vw 33 sh	74 m 59 m 39 w	67 sh 49 w 41 sh 37 vw	65 vs 53 s 45 w, sh	65 sh 50 w 39 vw	
					32 vvw	

^a A_{1g} , B_{1g} , B_{2g} , and E_g are Raman-active modes and A_{2u} and E_u are IR-active modes. ^b Description of band intensities: vs, very strong; s, strong; m, medium; w, weak; vvw, very very weak; vvw, very very weak; sh, shoulder. ^c Solid-state splittings of degenerate CN stretching vibrations.

is naturally attributed to the “lanthanide contraction”, namely, similar sizes of the third-row d-block metal atoms and their second-row counterparts. The effect is now considered to be the result of both shell-structure and relativistic effects.²⁹ The latter factor can be particularly large for a heavy element such as platinum, having an atomic number only one unit

less than that of gold, which experiences the largest relativistic contraction among the period 6 elements.³⁰ Thus, the ionic radii of divalent palladium and platinum cations in square-planar geometry are 0.78 and 0.74 Å, respectively; corresponding values for octahedral complexes are 1.00 and 0.94 Å.³¹ This can fully account for the ~0.03 Å difference

(29) Kaltsoyannis, N. *J. Chem. Soc., Dalton Trans.* **1996**, 1–11.

(30) Pyykkö, P. *Chem. Rev.* **1988**, 88, 563.

Table 5. Comparison of Experimental and Calculated (DFT; NCA^a) Fundamental Vibrational Wavenumbers Together with the PED

symmetry	$Tl_2Ni(CN)_4$			$Tl_2Pd(CN)_4$			$Tl_2Pt(CN)_4$			PED, %	assignment
	DFT	NCA	exp	DFT	NCA	exp	DFT	NCA	exp		
A_{1g}	2149	2134	2135	2172	2150	2151	2173	2158	2157	95 ν_1	ν_1 , CN sym str, $\nu_s(CN)$
	410	411	409	410	428	430	446	476	479	95 ν_2	ν_2 , MC sym str, $\nu_s(MC)$
	73	142	142	74	138	138	76	138	142	100 ν_3	ν_3 , MTI sym str, $\nu_s(MTI)$
A_{2g}	314			273			303				ν_4 , inactive
B_{1g}	2139	2118	2119	2159	2132	2133	2158	2136	2136	95 ν_5	ν_5 , CN str, $\nu(CN)$
	402	370	370	398	394	392	432	488	488	95 ν_6	ν_6 , MC str, $\nu(MC)$
B_{2g}	458	433	431	398	384	384	426	413	413	67 ν_7 , 33 ν_8	ν_7 , MCN out-of-plane lin bend, $\delta(MCN)$
	108	172	173	86	159	160	103	160	161	90 ν_8 , 10 ν_7	ν_8 , CMC deform, $\delta(CMC)$
E_g	287	311	310	240	302	303	282	328	328	Ni: 78 ν_9 , 22 ν_{10} Pd: 84 ν_9 , 16 ν_{10} Pt: 74 ν_9 , 26 ν_{10}	ν_9 , MCN in-plane lin bend, $\delta(MCN)$
	-95	83	96	-50	76	87	-36	82	83	Ni: 78 ν_{10} , 22 ν_9 Pd: 91 ν_9 , 9 ν_{10} Pt: 74 ν_9 , 26 ν_{10}	ν_{10} , TIMC deform, $\delta(TIMC)$
	446	422	422	395	430	430	439	470	469	Ni: 74 ν_{11} , 18 ν_{13} , 8 ν_{12} Pd, Pt: 86 ν_{11} , 13 ν_{13}	ν_{11} , MCN in-plane lin bend, $\delta(MCN)$
A_{2u}	167	165	158	133	142	146	114	137	136	Ni: 65 ν_{12} , 34 ν_{13} Pd, Pt: 83 ν_{12} , 12 ν_{13}	ν_{12} , MTI asym str, $\nu_a(MTI)$
	-95	109	120	38	119	119	60	106	116	Ni: 47 ν_{13} , 27 ν_{11} , 26 ν_{12} Pd: 75 ν_{13} , 16 ν_{12} Pt: 66 ν_{13} , 18 ν_{11} , 15 ν_{12}	ν_{13} , TIMC deform, $\delta(TIMC)$
	374			359			408				ν_{14} , inactive
B_{2u}	-90			-30			-36				ν_{15} , inactive
	2131	2118	2127, 2122	2152	2130	2138, 2122	2150	2131	2140, 2122	96 ν_{16}	ν_{16} , CN asym str, $\nu_a(CN)$
E_u	520	511	510	450	477	477	458	492	486	Ni: 72 ν_{17} , 18 ν_{18} , 7 ν_{19} Pd: 86 ν_{17} , 6 ν_{18} Pt: 94 ν_{17}	ν_{17} , MCN out-of-plane lin bend, $\delta(MCN)$
	410	412	413	384	384	384	403	408	409	Ni: 69 ν_{18} , 23 ν_{17} , 7 ν_{20} Pd: 75 ν_{18} , 16 ν_{19} , 9 ν_{17} Pt: 87 ν_{18} , 11 ν_{19}	ν_{18} , MC str, $\nu_a(MC)$
	108	110	135	83	121	135	99	113	124	Ni: 79 ν_{19} , 12 ν_{18} , 7 ν_{20} Pd: 77 ν_{19} , 19 ν_{18} Pt: 87 ν_{19} , 11 ν_{18}	ν_{19} , CMC deform, $\delta(CMC)$
	24	37		-18	34		-14	30		Ni: 92 ν_{20} , 7 ν_{19} Pd, Pt: 97 ν_{20}	ν_{20} , TIMC deform, $\delta(TIMC)$

^a NCA is normal coordinate analysis.**Table 6.** Refined Force Constants of the $Tl_2M(CN)_4$ Compounds in Internal Coordinates^{a-c}

		$Tl_2Ni(CN)_4$	$Tl_2Pd(CN)_4$	$Tl_2Pt(CN)_4$
stretching	K_{CN}	1652.8	1661.9	1664.9
	K_{MC}	187.0	211.4	289.8
	K_{MTI}	146.2	139.6	156.2
stretching–stretching	$F_{CN-CN'}$	2.8	3.3	1.9
	$F_{CN-CN''}$	4.9	5.3	7.6
	$F_{MC-MC'}$	23.5	10.8	3.8
	$F_{MC-MC''}$	35.8	59.0	38.0
	F_{CN-MC}	14	5	16
	$F_{CN-MC'}$	-3	-4	4-3
	$F_{MTI-MTI}$	95.0	95.7	86.2
bending	H_α^a	22.3	39.3	79.3
	H_φ	54.1	47.2	49.7
	H_β	74.6	72.1	78.6
	H_γ	30.7	28.3	34.5
	$h_{\alpha\alpha\alpha\alpha}$	-0.4	-1.6	-2.8
	$h_{\varphi\varphi\varphi\varphi}$	25.9	17.6	7.3
	$h_{\beta\beta\beta\beta}$	-15.0	-19.4	-23.9

^a α indicates in-plane and φ out-of-plane M–C–N linear bendings, β CMC indicates deformation, and γ TIMC deformation. ^b Single prime indicates cis and double prime indicates trans coordinates. ^c Stretch force constants are given in N/m, stretch–bend constants in 10^{-6} N/rad, and bend–bend constants in 10^{-16} Nm/rad².

in the Pd–Tl and Pt–Tl distances in the $Tl_2M(CN)_4$ compounds. A similar difference between the Pd–Tl and Pt–Tl bond lengths (2.9411 and 2.922 Å, respectively) has been

observed for a pair of isostructural compounds $Tl_2M_4Se_6$ (M = Pd, Pt).³²

Ab initio calculations of molecular $Tl_2Pt(CN)_4$ give a Pt–Tl bond distance of 2.877 Å,⁴ similar to our best ADF result of 2.813 Å, with both values including spin–orbit effects and both substantially shorter than the experimental value reported. It was suggested⁴ that electrostatic forces between a positively charged thallium ion and five negatively charged nitrogen atoms of the neighboring $[Pt(CN)_4]^{2-}$ units in the crystal structure (Figure 2) could effectively reduce the Pt–Tl interaction, resulting in considerable elongation of the metal–metal bond. This electrostatic lengthening of the M–Tl bond due to Tl–N interactions can also be expected to occur in the case of the isostructural $Tl_2Ni(CN)_4$ and $Tl_2Pd(CN)_4$ compounds (Figure 2). ADF calculations of isolated $Tl_2M(CN)_4$ molecules (without inclusion of spin–orbit coupling) give distances between the metal atoms of 2.674, 2.804, and 2.840 Å for M = Ni, Pd, and Pt, respectively, all 0.3–0.4 Å shorter than the experimental values (Table 2).

(31) Shannon, R. D. *Acta Crystallogr.* **1976**, A32, 751–767.

(32) (a) Bronger, W.; Bonsmann, B. Z. *Anorg. Allg. Chem.* **1995**, 621, 2083–2088. (b) No notable metal–metal bonding between the thallium(I) and platinum(IV) ions in the structure is found: the Tl–Pt⁴⁺ distance is 4.636, 4.719, and 4.895 Å for X = S, Se, and Te, respectively.

Table 7. Force Constants of the $K_2[M(CN)_4]$ Compounds in Internal Coordinates^{a-c}

	$K_2[Ni(CN)_4]$	$K_2[Pd(CN)_4]$	$K_2[Pt(CN)_4]$
K_{CN}	1656	1667	1650
K_{MC}	252	271	336
$F_{CN-CN'}$	2	3	4
$F_{CN-CN''}$	9	8	23
$F_{M-MC'}$	-3	-1	2
$F_{MC-MC''}$	19	23	12
F_{CN-MC}	1	-4	-5
$F_{CN-MC'}$	0	-2	-3
$F_{CN-MC''}$	0	-4	5
H_α	42	37	40
H_φ	35	(37)	44
$h_{\varphi\varphi\varphi\varphi}$	10	(12)	14

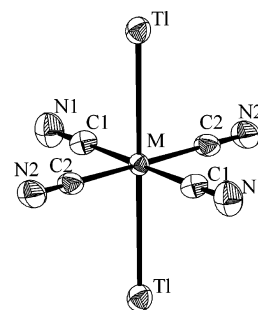
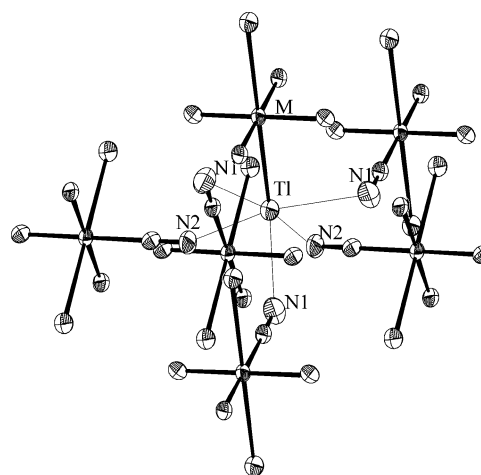
^a α indicates in-plane and φ out-of-plane M–C–N linear bendings.

^b Double prime indicates trans coordinates. ^c Stretch force constants are given in N/m, stretch–bend constants in 10^{-6} N/rad, and bend–bend constants in 10^{-16} Nm/rad².

We confirmed the great sensitivity of the M–Tl distances to Tl–N contacts by doing geometry optimizations of all three compounds that included solvation effects through the COSMO model within ADF. The optimized M–Tl bond distances with solvation (but not spin–orbit) effects included are 2.922, 3.123, and 3.086 Å for M = Ni, Pd, and Pt, respectively, all within 0.14 Å of the corresponding experimental values for the crystalline solids. This finding supports the suggestion⁴ that electrostatic Tl–N interactions in the crystals of these compounds are responsible for the substantially longer experimental Tl–M distances compared with the values calculated for isolated, molecular species. The incorporation of solvation effects also allows the effects of Tl–N interactions to be computationally mimicked in a simple way that retains the full D_{4h} molecular symmetry of these compounds.

The results for $Tl_2M(CN)_4$ are in agreement with the experimental data on the Pt–Tl bond distances in the isostructural series of compounds $Tl_2Pt_4X_6$ ($Tl_2Pt^{4+}Pt^{2+}_3X_6$, where X = S, Se, Te).^{32a} The coordination geometry of the Pt^{II} ions^{32b} in the compounds is very close to that in $Tl_2M(CN)_4$: a pseudo-octahedron with the two monovalent thallium ions in trans positions and the four chalcogen atoms in the equatorial plane. Substantial shortening of the metal–metal separation along the chalcogen group (3.002, 2.928, and 2.876 Å for the S, Se, and Te compounds, respectively) probably results from the corresponding decrease of the electrostatic interactions between the thallium atom and the chalcogens coordinated to the platinum of the adjacent polyhedra. This would account for the smooth variation of these distances with chalcogen electronegativity ($\chi_\alpha = 2.49$, 2.31, and 2.08 for S, Se, and Te, respectively).³³

The influence of the coordination environment of the thallium atom in the crystal structure on the thallium–palladium distances can be seen in the compounds $Tl_2Pd_4Se_6$ ^{32a} and Tl_2PdSe_2 ,³⁴ both containing Tl_2PdSe_4 fragments with a linear Tl–Pd–Tl entity. In the former case, the thallium atom has three adjacent palladium atoms (Tl–Pd = 2.941 Å) and three selenium atoms (Tl–Se = 3.154 Å),

**Figure 1.** Molecular structure of the isostructural compounds $Tl_2M(CN)_4$ (M = Ni, Pd, Pt).**Figure 2.** Coordination environment of the thallium ion in the crystal structure of $Tl_2M(CN)_4$ (M = Ni, Pd, Pt).

whereas in the latter case, the thallium atom is linked only to one palladium atom (Tl–Pd = 2.923 Å) and an irregular environment of eight selenium atoms (Tl–Se = 3.250–3.916 Å). Thus, the shorter metal–chalcogen contacts result in the lengthening of the metal–metal bonds, although the number of palladium atoms bound to thallium also probably has an impact on the Tl–Pd bonding.

Fully consistent with the considerations discussed above on the influence of the electrostatic Tl–X interactions on the Tl–M bonds, the metal–metal distances in the chalcogen compounds of platinum and palladium are significantly shorter, compared with the Tl–Pt and Tl–Pd distances (3.140 and 3.1733 Å, respectively) in $Tl_2M(CN)_4$ molecules. It is natural to attribute this lengthening to a stronger Tl–N interaction ($\chi_\alpha(N) = 3.12$)³³ than that in the Tl–X case (X = S, Se, Te).

Vibrational Spectroscopic and Force-Field Study of the $Tl_2M(CN)_4$ (M = Ni, Pd, Pt) Compounds. Tl–M Bond Strength. Assignment of the bands in the IR and Raman spectra of the solid $Tl_2M(CN)_4$ compounds is almost straightforward when dealing with stretching C–N, M–C and bending N–C–M, C–M–C vibrations (see Table 4, Figure 3, and Supporting Information Figures S2 and S3). It is also greatly facilitated by the DFT computation of the theoretical frequencies for the $Tl_2M(CN)_4$ molecules as well as the literature data on the parent $K_2[M(CN)_4]$ compounds (vide infra). The assignment becomes, however, more challengeable in the low-frequency region of the vibrational spectra, below 200 cm^{-1} (cf. Figure 3), where characteristic

(33) Nagle, J. K. *J. Am. Chem. Soc.* **1990**, *112*, 4741–4747.

(34) Klepp, K. O. *J. Less-Common Met.* **1985**, *107*, 147–153.

bands due to the metal–metal stretching vibrations are expected (see, e.g., ref 35). One can expect that one of the vibrations in the sets of the bands in ranges of 96–173, 87–160, and 83–161 cm^{-1} for $M = Ni, Pd,$ and Pt , respectively, belongs to the symmetric $Tl-M$ stretch in the $Tl_2M(CN)_4$ compounds (see Figure 3).

In contrast to the unambiguous assignment of the stretching $Tl-Pt$ vibration in the Raman spectra of solution species of the family of binuclear complexes $[(NC)_5Pt-Tl(CN)_n]^{n-}$ exhibiting a strong polarized band in the region of 159–164 cm^{-1} ,³⁶ no bands appear in the spectra of aqueous solutions of the $Tl_2M(CN)_4$ compounds below 300 cm^{-1} because of complete dissociation of the compounds into Tl^+ and $[M(CN)_4]^{2-}$ ions. The cleavage of the $Tl-M$ bonds in the aqueous solutions of the $Tl_2M(CN)_4$ compounds clearly shows that the metal–metal bonding is weaker than that in the case of previously studied binuclear $Tl-Pt$ complexes.

Another indication of the relative weakness of the $Tl-M$ bonding in the $Tl_2M(CN)_4$ compounds is provided by ^{195}Pt NMR magic angle spinning (MAS) spectra of $Tl_2Pt(CN)_4$. The one-bond $^{195}Pt-^{205}Tl$ spin–spin coupling constant in this species is only 1400 Hz³⁷ as compared with 38800–71100 Hz for the binuclear $[(NC)_5Pt-Tl(CN)_n]^{n-}$ species.^{36a,38}

To assess the strength of the $Tl-M$ bond in the series of $Tl_2M(CN)_4$ compounds from their vibrational spectra, a frequency of the $Tl-M$ stretching vibration is needed. We attempted to assign a $Tl-M$ stretch in the set of low-frequency bands in the Raman spectra of the $Tl_2M(CN)_4$ compounds based on both theoretical vibrational spectra of the molecules (Table 5) and assessment of the force constant of the bond, $K(Tl-M)$. If a higher frequency band, 173, 160, and 161 cm^{-1} for the compounds of Ni, Pd, and Pt, respectively, is then considered to be a symmetric stretching frequency of the $Tl-M$ bond, the rigorous calculations result in corresponding force constants, $K(Tl-M)$, of 195, 186, and 215 N/m, respectively. The values are unreasonably high for the rather long $M^{II}-Tl^I$ bonds of 3.06, 3.17, and 3.14 Å for $M = Ni, Pd,$ and Pt , respectively. Thus, for example, in the case of a short and nonbuttressed $Pt^{II}-Tl^{III}$ bond in the series of bimetallic complexes $[(NC)_5Pt-Tl(CN)_n]^{n-}$, the substantially shorter metal–metal distances, 2.60–2.64 Å, correspond to the $K(Tl-Pt)$ 174–156 N/m values, whereas the assignment of the $Tl-Pt$ stretching bands is straightforward (vide supra).^{36b,39} The literature data on the force constants for similar “trinuclear” $M-M'-M$ metal systems exhibit K

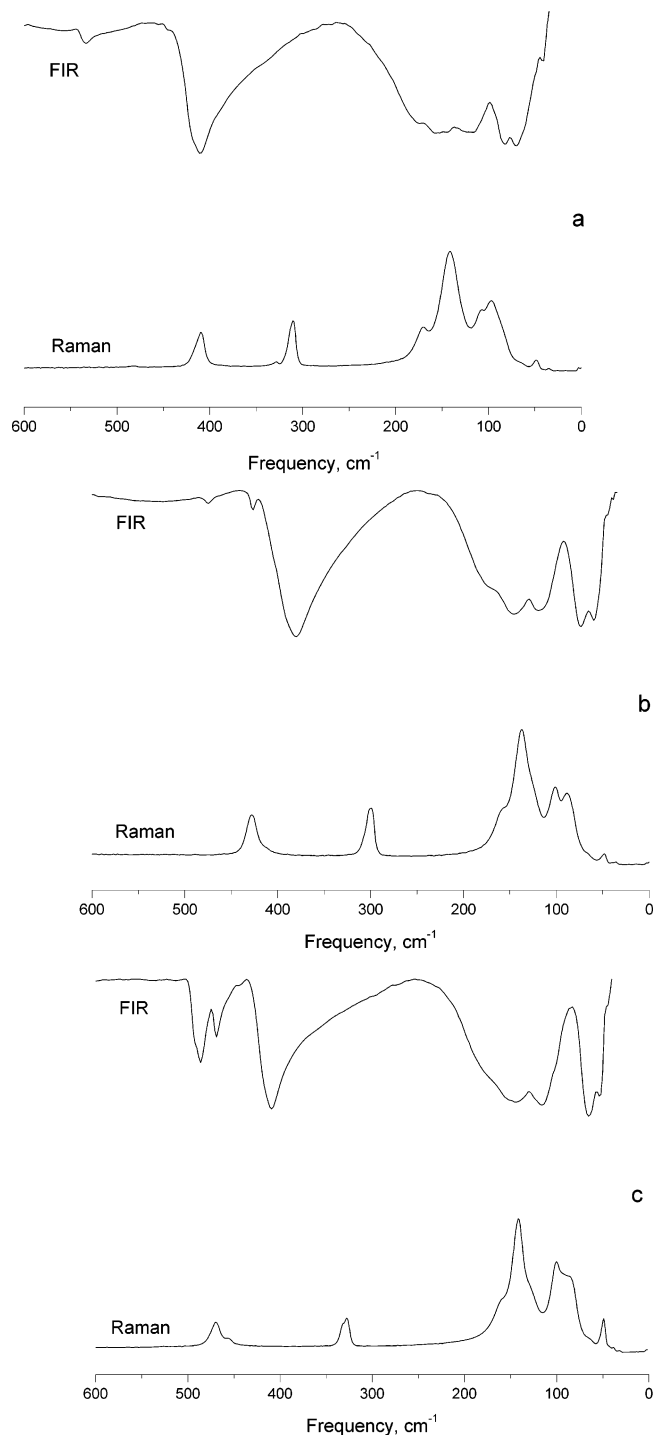


Figure 3. Low-frequency regions of the Raman and far-infrared spectra of $Tl_2M(CN)_4$ compounds: parts a, b, and c show spectra for $M = Ni, Pd,$ and Pt , respectively.

values below 130 N/m.^{35c} Therefore, we suppose that this band cannot arise from the $Tl-M$ symmetric stretch, and we assign it instead to a $C-M-C$ (B_{2g}) bending vibration.

On the contrary, the use of the set of bands lower than 100 cm^{-1} (96, 87, and 83 cm^{-1} for Ni, Pd, and Pt, respectively) leads to rather low values of the $M-Tl$ force constants (ca. 100 N/m), even for relatively weak metal–metal bonds in the case of the $Tl_2M(CN)_4$ compounds. Therefore, we attribute the $M-Tl$ stretching vibrations to the set of frequencies at 142(Raman)/161(IR), 138/146, and

- (35) (a) Shriver, D. F.; Cooper, C. B. In *Advances in Infrared and Raman Spectroscopy*; Clark, R. J. H., Hester, R. E., Eds.; Heyden: London, 1980; Vol. 6, pp 127–157. (b) Cotton, F. A.; Walton, R. A. *Multiple Bonds Between Metal Atoms*, 2nd ed.; Clarendon Press: Oxford, 1993. (c) Nakamoto, K. *Infrared and Raman Spectra of Inorganic and Coordination Compounds*, 5th ed.; Wiley-Interscience: New York, 1997; Vol. A.
- (36) (a) Maliarik, M.; Berg, K.; Glaser, J.; Sandström, M.; Tóth, I. *Inorg. Chem.* **1998**, *37*, 2910–2919. (b) Jalilehvand, F.; Maliarik, M.; Sandström, M.; Mink, J.; Persson, I. P. P.; Tóth, I.; Glaser, J. *Inorg. Chem.* **2001**, *41*, 3889–3899.
- (37) Thouvenot, R.; Nagle, J., unpublished data.
- (38) Apart from the strength of the metal–metal bond, $^1J(^{195}Pt-^{205}Tl)$ strongly reflects the variation of s character in the $Pt-Tl$ bond, which differs substantially for the complexes of Tl^I and Tl^{III} .
- (39) Jalilehvand, F.; Eriksson, L.; Glaser, J.; Maliarik, M.; Sandström, M.; Mink, J.; Tóth, I.; Tóth, J. *Chem.—Eur. J.* **2001**, *7*, 2167–2177.

Table 8. Mulliken Orbital Populations of $\text{Tl}_2\text{M}(\text{CN})_4$ Molecules Derived from ADF Calculations (Solvation and Spin–Orbit Effects Not Included) for the HOMO a_{1g} and LUMO a_{2u} (a_{2u} in All Cases)^a

	$\text{Tl}_2\text{Ni}(\text{CN})_4$	$\text{Tl}_2\text{Pd}(\text{CN})_4$	$\text{Tl}_2\text{Pt}(\text{CN})_4$
HOMO a_{1g} (energy, eV)	23 a_{1g} (−7.55)	25 a_{1g} (−7.92)	27 a_{1g} (−8.12)
Mulliken populations of a_{1g} MO with values $\geq 10\%$	68% Ni (66% 3 d_{z^2})	41% CN (25% N 2 p_y)	34% CN (22% N 2 p_y)
	20% Tl (14% 6s)	32% Pd (22% 4 d_{z^2})	33% Pt (23% 5 d_{z^2})
	12% CN	24% Tl (17% 6 p_z)	29% Tl (20% 6 p_z)
LUMO (energy, eV)	18 a_{2u} (−4.46)	19 a_{2u} (−4.37)	21 a_{2u} (−4.48)
Mulliken populations of a_{2u} MO with values $\geq 10\%$	52% Tl (38% 6 p_z)	60% Tl (52% 6 p_z)	78% Tl (72% 6 p_z)
	25% CN (20% N 2 p_z)	20% Pd (16% 6 p_z)	20% CN (16% N 2 p_z)
	23% Ni (22% 4 p_z)	20% CN (15% N 2 p_z)	
$E(a_{2u}) - E(a_{1g})$, eV	3.09	3.55	3.64

^a Orbital energies and orbital energy differences are also given. All values were calculated at the geometry-optimized distances and with QZ4P basis sets for all atoms.

142/136 cm^{-1} for Ni, Pd, and Pt, respectively. This results in rather reasonable values for the force constants, 139–156 N/m (see Table 6). The bands at 96, 87, and 83 cm^{-1} for Ni, Pd, and Pt, respectively, in the Raman spectra and at 114, 129, and 116 cm^{-1} for Ni, Pd, and Pt, respectively, in the IR spectra of the compounds were attributed to TIMC deformation modes (E_g) for Raman-active and A_{2u} for IR-active vibrations).

The strength of the metal–metal bonding in the series of $\text{Tl}_2\text{M}(\text{CN})_4$ compounds increases in the order Pd < Ni < Pt. The weakest M–Tl bond occurs in $\text{Tl}_2\text{Pd}(\text{CN})_4$ and, as expected, corresponds to the longest M–Tl bond distance, whereas the largest metal–metal force constant, for $\text{Tl}_2\text{Pt}(\text{CN})_4$, is explained in terms of the strongest interaction between the heavy neighboring elements of the sixth row of the periodic table, platinum and thallium. This probably can be attributed to the most effective overlapping of orbitals strongly contributing to the metal–metal bonding, namely, the nearly isoergic thallium 6 p_z and platinum 5 d_{z^2} orbitals (vide infra; see Table 8).⁴⁰

The characteristic stretching vibration of the cyano group, $\nu_s(\text{CN})$, as well as the metal–carbon stretch, $\nu_s(\text{MC})$, also provide valuable information on the bonding situation within $\text{Tl}_2\text{M}(\text{CN})_4$ molecules, especially in comparison with the data on the parent $\text{K}_2[\text{M}(\text{CN})_4]$ compounds. In contrast to the case of $\nu(\text{Tl–M})$, the assignment of the C–N and M–C vibrations in the Raman spectra of the thallium tetracyanometalates is unambiguous and was done in accordance with the procedure described by Kubas and Jones.²² Although in the series of the $\text{Tl}_2\text{M}(\text{CN})_4$ compounds the calculated force constants of the C–N bond increase somewhat from nickel to platinum (Table 6), the corresponding values of the $\text{K}_2\text{[M}(\text{CN})_4\text{]}$ salts show that bonding in the cyanide group is not influenced by the nature of the central metal atom (Table 7). The C–N bonding is not sensitive to the metal–metal interactions in the tetracyanometalate compounds; the force constants are almost the same for the Tl–M–Tl and –M–M–M– cases. The largest discrepancy observed for the two types of platinum compounds is less than 1%.

The strength of the metal–carbon bond in the series of $\text{Tl}_2\text{M}(\text{CN})_4$ molecules increases from nickel to platinum following a similar trend for the $\text{K}_2[\text{M}(\text{CN})_4]$ compounds (Table 6). The $K(\text{M–C})$ values are substantially lower in the case of thallium salts. Some destabilization of the metal–carbon bond obviously results from M–Tl bonding. When studying potassium salts of the $[\text{M}(\text{CN})_4]^{2-}$ anion (M = Ni, Pd, Pt) both in solution and in the solid state, Kubas and Jones concluded that the Pt–C bond had both greater σ and π bond strength than either of the components in the case of nickel and palladium compounds.²² One can suppose that because of the much shorter Tl–Pt interatomic separation (3.14 Å) in the thallium compound, compared with the Pt–Pt distance (3.48 Å) in the potassium salt,⁴¹ the π component of the Pt–C bond is probably more strongly affected by platinum–thallium bonding.

Theoretical ADF vibrational wavenumbers together with experimental and potential energy distribution (PED) values are given in Table 5. The agreement between the experimental and theoretical values is quite good, particularly considering that the theoretical values were obtained for discrete molecular $\text{Tl}_2\text{M}(\text{CN})_4$ species at the shorter Tl–M theoretical distances. This provides strong support for the proposed symmetry and force-constant assignments.

Metal–Metal Bonding in the Tl–M Entity (M = Ni, Pd, Pt). No compounds with bonds between thallium and nickel atoms have hitherto been reported. The relatively short Tl–Ni separation in the structure of $\text{Tl}_2\text{Ni}(\text{CN})_4$ can be considered as the first example of such a bond. The number of compounds incorporating Tl–M bonds increases down group 10 of the periodic table. Formation of the metal–metal bond between palladium and thallium ions was reported for three compounds with electron configuration 4 d^8 –6 s^2 (Pd^{II}–Tl^I). Apart from the two above-mentioned palladium selenide salts, $\text{Tl}_2\text{Pd}_4\text{Se}_6$ (Pd–Tl = 2.941 Å)^{32a} and Tl_2PdSe_2 (Pd–Tl = 2.923 Å),³⁴ a cyanide compound was also prepared, $[\text{Tl}(\text{crown-P}_2)\text{Pd}(\text{CN})_2](\text{PF}_6)\cdot\text{CHCl}_3$ (Pd–Tl = 2.897 Å).⁴² The former two structures appear to be very similar to that of $\text{Tl}_2\text{Pd}(\text{CN})_4$. Instead of the usual

(40) This is also illustrated by nearly equal contribution of metal orbitals (Tl 6 p_z and Pt 5 d_{z^2} both ~30%) to the HOMO (a_{1g} in all three compounds) for $\text{Tl}_2\text{Pt}(\text{CN})_4$ (see Table 8). The HOMO exhibits also the largest degree of Tl 6 p_z orbital involvement for $\text{Tl}_2\text{Pt}(\text{CN})_4$.

(41) Washecheck, D. M.; Peterson, S. W.; Reis, A. H.; Williams, J. M. *Inorg. Chem.* **1976**, *15*, 74–78.

(42) Balch, A. L.; Davis, B. J.; Fung, E. Y.; Olmstead, M. M. *Inorg. Chim. Acta* **1993**, *212*, 149–156.

infinite chains of palladium atoms with relatively short (3.16 Å) $\cdots Pd \cdots Pd \cdots Pd \cdots$ separations found in the selenopalladates of alkali metals,⁴³ the thallium compounds contain trans Tl_2PdSe_4 polyhedra with substantially stronger metal–metal interactions. The unusual structure of the salt of monovalent thallium with a linear $Tl–Pd–Tl$ fragment was attributed to the stereochemical activity of the lone pair allowing the repulsion between palladium and thallium in the compound to be overcome.³⁴

A number of palladium–thallium compounds with $4d^{10}–6s^2$ electron configuration of the $Pd^0–Tl^I$ metal–metal entity also have been reported. Two compounds of palladium metallocryptands encapsulating Tl^+ ions were prepared.^{40b} The palladium is in its zerovalent oxidation state, and the crystal structures of the complexes $[Pd_2Tl(P_2phen)_3]^+$ and $[Pd_2Tl(P_2bpy)_3]^+$ exhibit $Pd–Tl$ separations of 2.7914 and 2.7678 Å, respectively. In contrast to the compounds with $Pd–Tl$ bonds described above, here the thallium atom “binds” two palladium atoms in a ligand-supported $Pd–Tl–Pd$ entity. A modification of the former complex, where Au^I replaces one palladium atom, has been also reported recently.⁴⁴ In the structure of the trinuclear $Pd–Tl–Au$ species, Pd and Au atoms are positionally disordered and the $Pd–Tl$ separations range from 2.673 to 2.796 Å. A $Tl^I–(Pd_3)_2$ sandwich compound with six $Pd–Tl$ distances in the range of 2.820–3.119 Å also has been prepared.⁴⁵

Three types of bonding situations occurring between platinum and thallium atoms in heteronuclear compounds can be distinguished, depending on the formal oxidation state of the metal atoms: $5d^{10}–6s^2$ ($Pt^0–Tl^I$), $5d^8–6s^2$ ($Pt^{II}–Tl^I$), and $5d^8–6s^0$ or $5d^8–5d^{10}$ ($Pt^{II}–Tl^{III}$). In most cases it is impossible to assign the oxidation state of the metal atom in the heterometallic compound with a metal–metal bond to a certain discrete value because of apparent electron redistribution accompanying direct bonding. It is more correct to use the sum of the formal oxidation states of the coupled metals instead. The bond distances between these atoms in the compounds can be summarized as follows: $Pt^0–Tl^I$ (2.77–3.13 Å),^{40b,44–46} $Pt^{II}–Tl^I$ (2.80–3.51 Å),^{1,32a,47} $Pt^{II}–Tl^{III}$

(2.698–2.708 Å),⁴⁸ and $Pt^{II}–Tl^{III}$ (2.573–2.638 Å).^{36b,39,49} Considering compounds of divalent platinum, it is obvious that the $Pt–Tl$ bond becomes shorter when the oxidation state of thallium increases from Tl^I to Tl^{III} , which is consistent with the decreasing size of the thallium cation and with increased electron-acceptor properties of thallium.

As was shown above for the $Pt^{II}–Tl$ compounds incorporating thallium in different oxidation states, the shortening of the $Pt–Tl$ bond is also accompanied by a shift of the metal–metal symmetric stretching vibration to higher frequencies and a corresponding increase of the force constant. One can expect that similar strengthening of the $M^{II}–Tl$ bond for oxidation states of thallium higher than +1 will occur for the compounds of nickel and palladium, as well. Thus, the formation of the metal–metal bond in the $Ni^{II}–Tl^{III}$ and $Pd^{II}–Tl^{III}$ entities seems very probable.

The ADF-calculated Voronoi atomic charges (spin–orbit effects included) for M in isolated $Tl_2M(CN)_4$ molecules at the shorter, geometry-optimized $M–Tl$ distances are 0.17, 0.51, and 0.29 for $M = Ni, Pd,$ and Pt , respectively, remaining nearly unchanged at 0.19, 0.50, and 0.29, respectively, upon incorporation of solvation effects and at the longer experimental $M–Tl$ bond distances. Not surprisingly, the calculated Tl charges, on the other hand, show a much greater dependence on both the $M–Tl$ bond distance and solvation, increasing from 0.58, 0.56, and 0.58 (no solvation and short $M–Tl$ geometry-optimized distances) for $M = Ni, Pd,$ and Pt , respectively, to 0.65 for all three compounds at the longer, experimental $M–Tl$ distances (no solvation effects), to 0.77, 0.76, and 0.75, respectively, upon incorporation of solvation effects at the longer experimental $M–Tl$ bond distances. The large positive charges calculated for Tl under the latter conditions indicate that ionic attractions between Tl^I and $M(CN)_4^{2-}$ are important but not dominant in these crystalline compounds. Otherwise, the Tl^I atoms would, like K^+ ions in $K_2[M(CN)_4]$ salts, be expected to bond to the negatively charged N atoms instead of the positively charged M atoms.

Optical Features of the Metal–Metal Bond. The presence of direct platinum(II)–thallium(I) bonds in compounds is often associated with intense photoluminescence.^{20,47a,d,e,50,51} Depending on the compound (or ion in solution), emission bands associated with the metal–metal bond are observed in a wide range of wavelengths between 316 and 678 nm. Crystals of $Tl_2Pt(CN)_4$ show an intense blue luminescence (444 nm) at room temperature when irradiated in the near-ultraviolet region.¹ The absorption spectrum of the compound

(43) Bronger, W.; Rennau, R.; Schmitz, D. *Z. Anorg. Allg. Chem.* **1991**, *597*, 27–32.

(44) Catalano, V. J.; Malwitz, M. A. *J. Am. Chem. Soc.* **2004**, *126*, 6560–6561.

(45) Mednikov, E. G.; Dahl, L. F. *Dalton Trans.* **2003**, 3117–3125.

(46) (a) Ezomo, O. J.; Mingos, M. P.; Williams, I. D. *J. Chem. Soc., Chem. Commun.* **1987**, 924–925. (b) Hao, L.; Vittal, J. J.; Puddephatt, R. J. *Inorg. Chem.* **1996**, *35*, 269–270. (c) Catalano, V. J.; Bennett, B. L.; Muratidis, S.; Noll, B. C. *J. Am. Chem. Soc.* **2001**, *123*, 173–174. (d) Stadnichenko, R.; Sterenberg, B. T.; Bradford, A. M.; Jennings, M. C.; Puddephatt, R. J. *J. Chem. Soc., Dalton Trans.* **2002**, 1212–1216.

(47) (a) Balch, A.; Rowley, S. P. *J. Am. Chem. Soc.* **1990**, *112*, 6139–6140. (b) Klepp, K. O. *J. Alloys Compd.* **1993**, *196*, 25–28. (c) Renn, O.; Lippert, B. *Inorg. Chim. Acta* **1993**, *208*, 219–223. (d) Uson, R.; Fornies, J.; Tomas, M.; Garde, R.; Merino, R. I. *Inorg. Chem.* **1997**, *36*, 1383–1387. (e) Ara, I.; Berenguer, J. R.; Fornies, J.; Gomez, J.; Lalinde, E.; Merino, R. I. *Inorg. Chem.* **1997**, *36*, 6461–6464. (f) Berenguer, J. R.; Fornies, J.; Gomez, J.; Lalinde, E.; Moreno, M. T. *Organometallics* **2001**, *20*, 4847–4851. (g) Song, H.-B.; Zhang, Z.-Z.; Hui, Z.; Che, C.-M.; Mak, T. C. W. *Inorg. Chem.* **2002**, *41*, 3146–3154. (h) Oberbeckmann-Winter, N.; Braunstein, P.; Welter, R. *Organometallics* **2004**, *23*, 6311–6318. (i) Stork, J. R.; Olmstead, M. M.; Balch, A. L. *J. Am. Chem. Soc.* **2005**, *127*, 6512–6513.

(48) Uson, R.; Fornies, J.; Tomas, M.; Garde, R.; Alonso, P. *J. Am. Chem. Soc.* **1995**, *117*, 1837–38.

(49) (a) Ma, G.; Kritikos, M.; Glaser, J. *Eur. J. Inorg. Chem.* **2001**, 1311–1319. (b) Ma, G.; Fischer, A.; Glaser, J. *Eur. J. Inorg. Chem.* **2002**, 1307–1314. (c) Ma, G.; Kritikos, M.; Maliarik, M.; Glaser, J. *Inorg. Chem.* **2004**, *43*, 4328–4340. (d) Zhen, W.; Liu, F.; Matsumoto, K.; Autschbach, J.; Le Guennic, B.; Ziegler, T.; Maliarik, M.; Glaser, J. *Inorg. Chem.* **2006**, *45*, 4526–4536.

(50) Nagle, J. K.; Brennan, B. A. *J. Am. Chem. Soc.* **1988**, *110*, 5931–5932.

(51) Clodfelter, S. A.; Doede, T. M.; Brennan, B. A.; Nagle, J. K.; Bender, D. P.; Turner, W. A.; LaPunzina, P. M. *J. Am. Chem. Soc.* **1994**, *116*, 11379–11386.

reveals a single band at 370 nm. The optical properties of the compound were attributed to Tl–Pt–Tl interactions.

Although we have not been able to find any reports of emission attributed to either Tl–Pd or Tl–Ni bonds, it could be expected that isostructural analogues of $\text{Tl}_2\text{Pt}(\text{CN})_4$, $\text{Tl}_2\text{Ni}(\text{CN})_4$, and $\text{Tl}_2\text{Pd}(\text{CN})_4$ might exhibit similar emission properties. The emission bands in the spectra of the $\text{Tl}_2\text{Ni}(\text{CN})_4$ and $\text{Tl}_2\text{Pd}(\text{CN})_4$ compounds are very weak, and the spectra are noisy (see Supporting Information, Figure S2). Moreover, neither the steady-state nor time-resolved luminescence spectra of the corresponding thallium(I) and potassium salts of either $[\text{Ni}(\text{CN})_4]^{2-}$ or $[\text{Pd}(\text{CN})_4]^{2-}$ anions show any notable differences (see Supporting Information, Figure S2). Excitation spectra of the pairs of salts are very similar as well (see Supporting Information, Figures S3 and S4). It can be concluded, therefore, that the optical properties of the $\text{Tl}_2\text{Ni}(\text{CN})_4$ and $\text{Tl}_2\text{Pd}(\text{CN})_4$ compounds are dominated by very weak emission features of the $[\text{M}(\text{CN})_4]^{2-}$ anion ($\text{M} = \text{Ni}, \text{Pd}$), rather than the Tl–M–Tl bonding, as in the case of strongly luminescent $\text{Tl}_2\text{Pt}(\text{CN})_4$.

TDDFT calculations (spin–orbit effects not included) of excitation energies for $\text{Tl}_2\text{Ni}(\text{CN})_4$, $\text{Tl}_2\text{Pd}(\text{CN})_4$, and $\text{Tl}_2\text{Pt}(\text{CN})_4$ for the theoretically calculated lowest-energy geometries with short Tl–M distances reveal lowest-energy spin-allowed $a_{1g} \rightarrow a_{2u}$ transitions at 4.08 eV (304 nm), 4.17 eV (297 nm), and 4.30 eV (288 nm), respectively. The corresponding energies of these transitions calculated at the longer experimental Tl–M distances (and including solvation effects but not spin–orbit effects) are 3.56 eV (348 nm), 3.93 eV (315 nm), and 4.10 eV (302 nm). Mulliken populations from DFT (not TDDFT) calculations (not including solvation or spin–orbit effects) of the a_{1g} and a_{2u} orbitals and their calculated energies (for the shorter theoretical distances) are given in Table 8. The highest-occupied a_{1g} orbital in all three compounds is of mixed Tl–M–CN character, with $\text{Tl}_2\text{Ni}(\text{CN})_4$ exhibiting the largest degree of $\text{M} nd_{z^2}$ orbital involvement and the least amount of CN character. The lowest-unoccupied a_{2u} orbital for all three compounds is largely Tl $6p_z$ in nature but with significant CN^- contributions, with only $\text{Tl}_2\text{Ni}(\text{CN})_4$ and $\text{Tl}_2\text{Pd}(\text{CN})_4$ calculated to have greater than 10% $\text{M} np_z$ character for this orbital. Therefore, the lowest-energy $a_{1g} \rightarrow a_{2u}$ spin-allowed transition (${}^1A_{1g} \rightarrow {}^1A_{2u}$) is calculated to possess significant metal-centered $\text{M} nd_{z^2} \rightarrow \text{Tl} 6p_z$ charge-transfer character. Calculations at the longer experimental M–Tl distances, including solvation effects, result in similar conclusions. Although now the HOMO is an a_{1g} orbital for $\text{Tl}_2\text{Ni}(\text{CN})_4$ and $\text{Tl}_2\text{Pd}(\text{CN})_4$, all three compounds have less than a 10% CN contribution to the highest-occupied a_{1g} orbital, and $\text{Tl}_2\text{Pd}(\text{CN})_4$ shows the largest $a_{1g} - a_{2u}$ energy difference (3.96 eV vs 3.18 and 3.78 eV for $\text{M} = \text{Ni}$ and Pt , respectively).

Absorption spectra for $\text{Tl}_2\text{M}(\text{CN})_4$ as crystalline suspensions in glycerol show absorbance onsets to shorter wavelengths appearing at about 400, 360, and 400 nm for $\text{M} = \text{Ni}, \text{Pd}$, and Pt , respectively. Consistent with the emission results discussed above, $\text{Tl}_2\text{Pt}(\text{CN})_4$ differs from the other two compounds, exhibiting a distinct maximum at 370 nm,¹ just below its onset. The lowest-energy TDDFT-calculated

transitions (at the experimental M–Tl distances and including both solvation and spin–orbit effects) occur at 3.31 eV (375 nm), 3.82 eV (325 nm), and 3.46 eV (358 nm) for $\text{M} = \text{Ni}, \text{Pd}$, and Pt , respectively, all $A_{1g} \rightarrow E_u$ in nature. The agreement between calculated and experimental values is reasonable, with the highest energy absorbance onset for $\text{Tl}_2\text{Pd}(\text{CN})_4$ reflected in the computational results. The relative values of the calculated $A_{1g} \rightarrow E_u$ spin–orbit excitation energies for the three compounds point to substantial $\text{M} nd_{z^2} \rightarrow \text{Tl} 6p_z$ character for these lowest-energy transitions. This is because both the calculated Voronoi atomic charge (see above) and the energy of the $A_{1g} \rightarrow E_u$ spin–orbit excitation are most positive for $\text{M} = \text{Pd}$. Further analysis of the optical properties of all three of these compounds must await a more thorough experimental and computational investigation, including a detailed consideration of the large effects of spin–orbit coupling in all three compounds.⁵²

Conclusions

The crystalline compounds $\text{Tl}_2\text{Ni}(\text{CN})_4$ and $\text{Tl}_2\text{Pd}(\text{CN})_4$ were prepared, and their X-ray crystal structures were refined. Both salts are isostructural with the previously reported $\text{Tl}_2\text{Pt}(\text{CN})_4$ compound. In contrast to the usual infinite columnar stacking of $[\text{M}(\text{CN})_4]^{2-}$ ions with short intrachain M–M separations, as found in salts of the tetracyanometalates of Ni^{II} , Pd^{II} , and Pt^{II} , the structure of these compounds is noncolumnar. The two Tl^I ions occupy axial vertices of a distorted pseudo-octahedron of the transition metal, $[\text{MTl}_2\text{C}_4]$, whereas the original square-planar coordination of the four carbon atoms of the cyano groups is retained. The Tl–M distances in the compounds are 3.0560(6), 3.1733(7), and 3.140(1) Å for the Ni^{II} , Pd^{II} , and Pt^{II} salts, respectively. The absence of a monotonic decrease of the Tl–M separations down this group of transition metals correlates well, with palladium having the largest ionic radius of the three metal atoms, both in square-planar and octahedral coordination environments. To the best of our knowledge, the short Tl–Ni distance in the $\text{Tl}_2\text{Ni}(\text{CN})_4$ compound is the first example of metal–metal bonding between these two metals in a molecular species.

The strength of the metal–metal bonds in the series of compounds $\text{Tl}_2\text{M}(\text{CN})_4$ was assessed by means of vibrational spectroscopy and theoretical DFT calculations. Rigorous calculations of the force constants were performed on the molecules in D_{4h} point group symmetry. The force constants of the Tl–M stretching vibration are 146, 140, and 156 N/m for the Ni^{II} , Pd^{II} , and Pt^{II} compounds, respectively. The strongest metal–metal bonding, found in the case of the Tl–Pt compound, is attributed to the most effective overlapping of orbitals strongly contributing to the metal–metal bonding, namely, the nearly isoergic thallium $6p_z$ and platinum $5d_{z^2}$ orbitals. A comparative study of the vibrational spectra of the family of $\text{K}_2[\text{M}(\text{CN})_4]$ ($\text{M} = \text{Ni}^{\text{II}}, \text{Pd}^{\text{II}}, \text{Pt}^{\text{II}}$) compounds, having a polymeric chain $-\text{M}-\text{M}-\text{M}-$ structure, showed that the C–N bonding is not sensitive to the metal–metal

(52) Wang, F.; Ziegler, T. *J. Chem. Phys.* **2005**, *123*, 194102.1–194102.10.

interactions. However, the M–C force constants are strongly affected by the Tl–M bonding and were found to be weakened by 20% for $Tl_2Pt(CN)_4$ compared with that of $K_2[Pt(CN)_4]$.

In contrast to $Tl_2Pt(CN)_4$, which exhibits strong luminescence attributed to the Tl–Pt–Tl entity, the nickel and palladium analogues are feebly luminescent. The emission features are associated with the $[M(CN)_4]^{2-}$ unit rather than the metal–metal bond. This difference most likely results from a complicated interplay of excited-state energies and radiative and nonradiative transitions among these various states.

Acknowledgment. We thank Dr. Lars Eriksson and Prof. Rolf Norrestam (Arrhenius Laboratory, Department of Physical, Inorganic and Structural Chemistry, Stockholm University, Sweden) for providing the opportunity to collect X-ray crystal data on the STOE IPDS diffractometer and for helpful discussions. We would like to thank Dr. René Thouvenot

(Laboratoire de Chimie des Métaux de Transition, Université P. et M. Curie, Paris, France) for providing unpublished data on the ^{195}Pt NMR MAS of the $Tl_2Pt(CN)_4$ compound. Financial support from the Royal Swedish Academy of Sciences is greatly acknowledged. J.K.N. thanks Bowdoin College for support, including a Porter Fellowship, and Prof. Evert Jan Baerends for his kind hospitality, during a sabbatical leave at the Free University of Amsterdam.

Supporting Information Available: Crystallographic information file for the single-crystal structure determinations of compounds **1** and **2**; experimental polycrystalline diffractograms and diffractograms calculated from the single-crystal data X-ray of the $Tl_2M(CN)_4$ ($M = Ni, Pt$) compounds; luminescence and excitation spectra of polycrystalline compounds $Tl_2M(CN)_4$ ($M = Ni, Pd$) in comparison with corresponding $K_2M(CN)_4$ compounds. This material is available free of charge via the Internet at <http://pubs.acs.org>. IC062092K